

Seismic behaviour of regular reinforced concrete plane frames with fiber reinforced concrete in joints

L. Candido¹  · F. Micelli¹

Received: 24 July 2017 / Accepted: 2 February 2018
© Springer Science+Business Media B.V., part of Springer Nature 2018

Abstract According to most of current design standards, the need for high strength and ductility of reinforced concrete frame structures is accomplished utilizing a high amount of transverse reinforcement in beam–column joints. Reinforcement congestion can be overcome by means of Fiber Reinforced Concrete and High Performance Fiber Reinforced Concrete, which are known to improve the structural performance of single structural members or beam–column joints. Through an extended numerical simulation, this paper elaborates the overall benefits of using fiber reinforced concrete materials in critical regions to the seismic behaviour of regular reinforced concrete frame structures. An extensive number of non-linear static and dynamic analyses with distributed plasticity and fibre sections are performed to compare the behaviour of simple reinforced concrete and mixed reinforced concrete/fiber reinforced concrete frames in terms of total base shear and fragility curves and failure mechanisms. Even if execution and technological aspects are beyond the scope of the present work, the use of fiber reinforced concretes in critical regions of mixed frames seems to improve the structural performance of reinforced concrete frames at a global level.

Keywords Earthquakes · Reinforced concrete · Fiber reinforced concrete · Frame structures · Incremental dynamic analysis · Pushover analysis

List of symbols

ρ	Reinforcement ratio
d_c	Lateral displacement of the control point (centroid of the top floor)
f_y	Steel strength at yielding

✉ L. Candido
leandro.candido@unisalento.it

F. Micelli
francesco.micelli@unisalento.it

¹ Department of Innovation Engineering, University of Salento, Via Per Arnesano, 73100 Lecce, Italy

E_s, E_{cm}	Moduli of elasticity of the steel and of the concrete
b	Strain-hardening ratio (ratio between post-yield and initial moduli)
w_u	Maximum crack opening accepted in structural design
$CMOD_1, CMOD_3$	Crack mouth opening displacements at the SLS and ULS
l_{cs}	Characteristic length of the element
ε_{SLS}	$CMOD_1/l_{cs}$
ε_{tu}	Ultimate tensile strain in uniaxial tension
R_{ck}, f_{ck}	Characteristic values of concrete compressive strength on cubes and cylinders
f_{cd}, f_{ctd}	Design values of concrete strength in compression and in tension (on cylinders)
$\varepsilon_{cu}, \varepsilon_{tu}$	Design values of concrete ultimate strains in compression and in tension
f_{yk}, f_{yd}	Characteristic and design values of steel strength in tension
ε_{sd}	Design value of steel ultimate strain in tension
K	Strength amplification factor for concrete
ε_{c0}	Design value of concrete compressive strain at the peak stress
Z	Strength reduction factor for confined concrete after the peak stress
$\varepsilon_{c1}, \varepsilon_{c1}$	Design values at the first point in concrete trilinear model
$\varepsilon_{c2}, \varepsilon_{c2}$	Design values at the second point in concrete trilinear model
$\varepsilon_{c3}, \varepsilon_{c3}$	Design values at the third point in concrete trilinear model
$\varepsilon_{t1}, \varepsilon_{t2}$	Tensile strain at zero stress, and ultimate strain in concrete trilinear model

1 Introduction

When large amounts of fibres are mixed in concrete, the resulting fiber reinforced concrete (FRC) material shows ductile behaviour both in compression and in tension, displaying tensile strain hardening or softening behaviour (Di Prisco et al. 2009). As a result, the use of fiber reinforced concrete significantly improves the structural performance of reinforced concrete (RC) members, not only under static and fatigue loading, but also under dynamic and earthquake loading. The presence of structural fibers in the concrete matrix enhances the ductility and dissipation properties of the material (Vasanelli et al. 2014; Yuan et al. 2013; Bayasi and Gebman 2002; Filiatrault et al. 1995; Henager 1977; Jiuru et al. 1992; Minelli and Plizzari 2013). Such properties make fiber reinforced concrete and high performance fiber reinforced concrete (HPFRC) highly damage-tolerant and especially suitable to be used in inelastic and joint regions, where high load bearing capacity and energy dissipation are required. The ability to absorb large inelastic deformations and to resist shear reversals during earthquake events is an additional important requirement fulfilled by FRC and HPFRC (Parra-Montesinos et al. 2005), whose improved tensile resistance and hardening increase structural shear strength, especially under multi-axial stresses. Mishra and Li (1995) found that mechanical properties of engineered cementitious composites (ECCs) in shear are similar to those in tension. Shannag et al. (2005) demonstrated that using steel FRC to replace conventional concrete in beam-column joints can significantly increase their seismic behaviour. In joint regions with weak shear reinforcement, the presence of HPFRCs can turn the failure mode from brittle (in shear) to ductile (Yuan et al.

2013). Similarly, a recent experimental campaign showed that using ECC in beam–column joints can significantly increase the seismic performance of lightly reinforced joints as well (Yuan et al. 2013). This finding was also proved by many researchers over the last decade (Li and Wang 2002; Fischer and Li 2002a, b, 2003). Hence, using FRC/HPFRC in the joint regions can be highly beneficial since it can (a) replace conventional concrete (always brittle in shear); (b) limit or avoid reinforcement congestion; and (c) improve the overall performance under sustained and cyclic loads. Several international design codes, including Eurocode 8 (2004) and the Italian Building Code (2008), referred to as NTC08 below, are well known for their rather conservative provisions concerning the items mentioned above, so that they often require an excessive amount of reinforcements, even in the design of low-ductility frames.

Therefore, the benefits of using HPFRC have been widely proven at a local level in many applications over the past decades. However, it is still an open question to what extent FRC and HPFRC can improve the global behaviour of RC frame structures, especially since the construction technology for on-site large-scale applications needs to be further developed. Within this framework, it is of major interest to investigate the potential global benefits of using fibre-reinforced concrete in the joint and inelastic regions of earthquake-resistant RC frames comparing the expected performances with those of plain-concrete structures. At the moment, such an ambitious investigation can be only carried out by means of numerical analysis to simulate the behaviour of RC frame structures. So, an extensive numerical campaign based on nonlinear static or dynamic analysis is performed, in order to describe the behaviour of the seismic-resistant RC plane frames commonly used in residential buildings, namely with two to four bays and two to eight storeys. Ordinary concrete mixes (C25/30 and C40/50) are adopted for frame members, while (high performance) fibre-reinforced mixes (FRC25/30, FRC40/50 and FRC80/85) are used in the critical locations and beam–column joints. The joint regions are modelled with or without rigid end-sections, and in-plane perfect stiffness of floors is introduced as well. The frames are designed according to the current Italian Building Code and Eurocode 8 (EC8). A diffused-plasticity model is adopted for frame members in nonlinear static and dynamic analyses.

It is noted that in the present paper (a) the word *joint* refers to the volume of intersection between beams and columns, and (b) the expression *inelastic regions* refers to the ending parts of beams and columns which are typically indicated as critical regions in design. In the paper, indeed, both joints and inelastic regions are referred to as *dissipative zones*, while the remaining parts of the structures are referred to as elastic regions or *frame members*. Furthermore, it is noted that a list of symbols is reported at the end of the paper.

2 Case studies and structural analysis

The numerical campaign performed in this study consists of an extended set of analyses concerning typical frames found in regular residential buildings. Different geometries, materials and modelling techniques are considered, in order to set up a rich database consisting of 216 specific cases, with six combinations of frame geometries (two- or four-bays and two-, four- or eight-floors). The inter-storey height is set at 3.30 m at all levels, while the distance between the columns is set at 5.00 m. Each frame is first considered to be entirely made of ordinary C25/30- or C40/50-grade plain concrete. Then three classes of FRC are simulated to replace plain concrete in the inelastic and joint regions: namely FRC25/25,

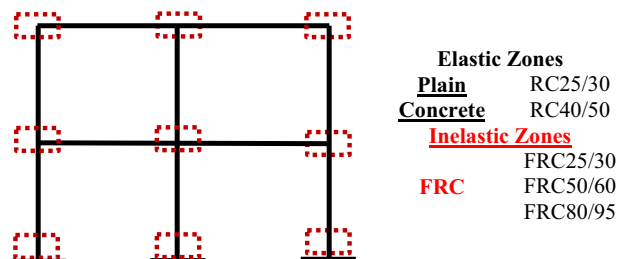
FRC50/60 and FRC80/95. Thus, six combinations of concrete grades are examined: namely RC25/RC25, FRC25/RC25, FRC50/RC25, FRC80/RC25 and FRC80/RC40. The first and second parts of each label refer to concrete compressive strength on cylinders to be adopted respectively in the dissipative zones and in the other parts of the structure. Figure 1 gives an illustration of the concept. The length of inelastic zones depends on the geometry of the elements; it is 66 and 45 cm respectively for beams and columns.

Beams and columns are modelled as beam elements, using a distributed-plasticity model. The joint zones are considered with or without rigid-end links for the entire lengths of the joint panel, as indicated by FEMA 356 (2000) in section 6.5.2.1. In the second case, the nonlinear behaviour of the beam–column panel is considered, modelling the panel zone as part of the column. Figure 2 illustrates the two modelling techniques for the beam–column joints. Furthermore, floors are assumed to have either perfect or no in-plane stiffness, in order to evaluate the effects that such constraint has on the global behaviour of the frames. The entire set of frames is subjected to nonlinear static and dynamic analyses performed according to Eurocode 8 and NTC08. Pushover analysis is performed by adopting either linear triangular or mass-proportional lateral-load profiles, while incremental dynamic analysis (IDA) is performed by using seven different natural spectrum-compatible earthquake records, according to EC8 section 4.3.3.4.3.

Buildings are designed to be earthquake-resistant in accordance with the low-ductility class (CDB) of RC frames (Eurocode 8 and NTC08). A peak ground-acceleration of 0.25 g, type A ground and regular topography (T1) are assumed for design purposes. The associated elastic response spectrum is based on a 10% probability to be overcome in 50 years, given a damping ratio as equal as 5%. Such seismic hazard, corresponding for instance to a site in the municipality of Reggio-Calabria (Italy), is greater than that of the 90% of Italian municipalities. Figure 3 illustrates the 7 spectrum-compatible accelerograms generated through the software SEISM-HOME (Rota et al. 2012), for horizontal topographic surface and return period as equal as 475 years. Column sections are assumed as square and their side length is dependent on the number of floors. The side length is equal to 400 and 450 mm respectively in two-storey and four-storey frame buildings (all floors). In the case of eight-storey frames, the column side length is equal to 500, 450 and 400 mm respectively for the first two sets of floors, for the second two sets of floors and for the last four floors.

The concrete cover is 30 mm thick and the reinforcement ratio in columns is approximately 1.55%. The sections are reinforced with 8Ø20, 10Ø20 and 12Ø20 bars respectively for sections size 400, 450 and 500 mm. Beam sections are always rectangular (sized 300 × 500 mm), reinforced with 8Ø16, respectively three to top and bottom sides and two on the lateral sides. For both columns and beams, stirrups spacing are assumed as equal to 12 and 18 cm respectively for the inelastic and elastic regions of members. For the intermediate and top floors, the loads are assigned respectively as follows: 7.2 and 5.6 kN/m² for dead

Fig. 1 Regions of application for PC or FRC in frames



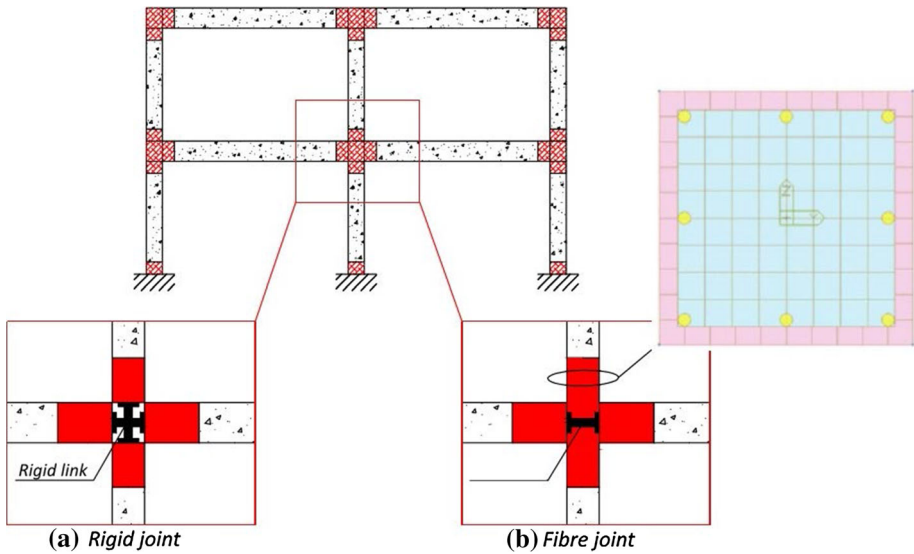


Fig. 2 Joint modelling techniques: **a** rigid-ends; **b** fibre-based joint

loads; and 2.0 and 1.1 kN/m² for live loads. Live loads for residential buildings are assigned according to the Italian Standards provisions in section 3.1.4, and Eurocode 1 (1991) section 6.3.1.1. The overall loads are applied in the seismic combination to the beams, assuming 2.5 m for the interspace between two successive frames. Columns are modelled as fully restrained at their base. Figure 4 illustrates the main geometrical properties of the investigated frame structures. The red dots are the control points (d_c) of each frame, which are used to draw top displacement in pushover or Incremental Dynamic Analysis (IDA) curves. Columns and beams are numbered from left to right. The analyses were run with MIDAS/Gen (2012) v.2.1. Among other software able to perform nonlinear analysis based on diffused plasticity models, the software turned out to be robust and user-friendly in displaying output information given the extensive number of analyses.

3 Material properties and constitutive models

Steel B450C is assumed for conventional reinforcements and two and three grades are assumed respectively for plain and fibre reinforced concretes. Table 1 reports the corresponding mechanical properties for concretes, as per Eurocode provisions. The analyses are based on design values of strengths and make use of fibre-based element formulation. Therefore, uniaxial stress–strain relations are needed. As for steel reinforcements, the constitutive model proposed by Menegotto and Pinto (1973) as modified by Filippou et al. (1983) is adopted with the following parameters: $f_y = 391$ MPa, $E_s = 210.000$ MPa and $b = 0.0052$ (Fig. 6a). As for concrete, different behaviours are expected for plain and fibre reinforced concretes, which differ mainly in the tensile properties. In design, plain concrete is assumed to have no tensile properties while fibre reinforced concrete has a post-cracking residual strength.

An ultimate tensile strain as equal as 3% is considered for FRCs in order to fit the post-cracking residual strength at ultimate strain according to the provisions offered by Model Code 2010 in section 5.6.4. Furthermore, the confinement effect has a role on compressive

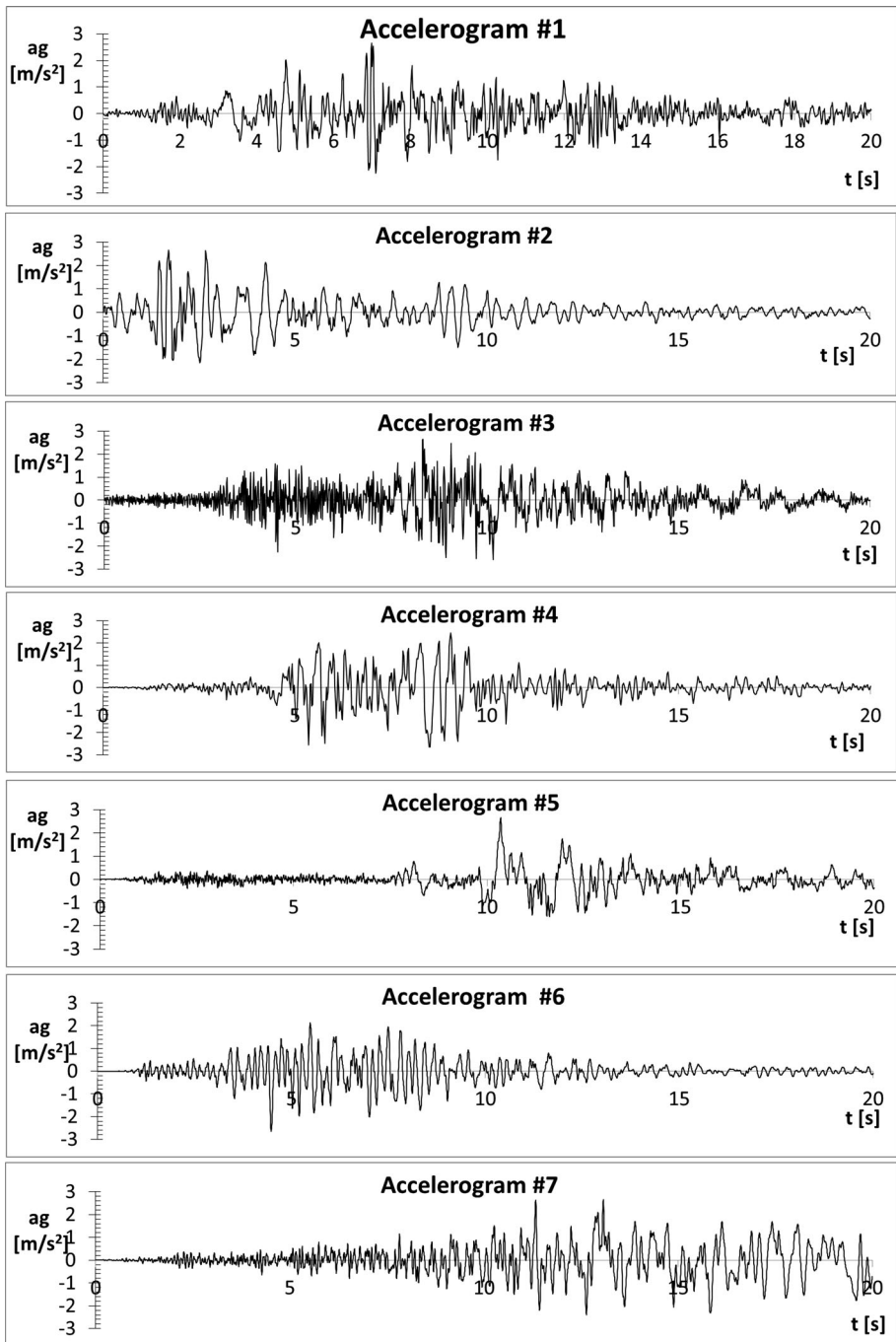


Fig. 3 Spectrum-compatible ground motions for the chosen site and $T_R = 475$ years

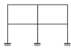

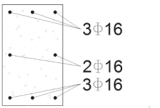
2-STOREY FRAMES							
2x2	4x2	Storey level	Columns		Beams		
			Size (cmxcm)	Steel bars	Size (cmxcm)	Steel bars	
		1	40x40	8Φ16	30x50	8Φ16	
		2	40x40	8Φ16	30x50	8Φ16	
4-STOREY FRAMES							
2x4	4x4	Storey level	Columns		Beams		
			Size (cmxcm)	Steel bars	Size (cmxcm)	Steel bars	
			1	45x45	10Φ20	30x50	8Φ16
			2	45x45	10Φ20	30x50	8Φ16
			3	45x45	10Φ20	30x50	8Φ16
4	45x45	10Φ20	30x50	8Φ16			
8-STOREY FRAMES							
2x8	4x8	Storey level	Columns		Beams		
			Size (cmxcm)	Steel bars	Size (cmxcm)	Steel bars	
			1	50x50	12Φ20	30x50	8Φ16
			2	50x50	12Φ20	30x50	8Φ16
			3	45x45	10Φ20	30x50	8Φ16
			4	45x45	10Φ20	30x50	8Φ16
			5	40x40	8Φ16	30x50	8Φ16
			6	40x40	8Φ16	30x50	8Φ16
Beams		7	40x40	8Φ16	30x50	8Φ16	
		8	40x40	8Φ16	30x50	8Φ16	
Other characteristics							
Interfloor Height				H _i	3.3	m	
Span Length				L _b	5	m	
Concrete Cover				c	3	cm	
In-plane floor stiffness				Off			

Fig. 4 Geometrical characteristics of investigated frames

behaviour as well. Consequently, different constitutive laws are assumed for confined and unconfined concrete regions. According to NTC08/Eurocodes, for unconfined concrete with grade lower than C50/60 the strain at reaching the maximum strength is $\epsilon_{c2} = 0.20\%$ and the ultimate strain is $\epsilon_{cu} = 0.35\%$, while for higher grades $\epsilon_{c2} = 0.20\% + 0.0085\%(f_{ck} - 50)^{0.53}$ and $\epsilon_{cu} = 0.26\% + 3.5\%[(90 - f_{ck})/100]^4$, where f_{ck} is the characteristic compressive cylinder strength of concrete at 28 days. Because no recommendation is provided for FRC, ϵ_{cu} is incremented by 0.3% taking into account the contribution of fibres, which is the minimum increment in the peak strain for FRC as derived by ACI 544.4R section 2.2. The effect of confinement on the constitutive law, as accounted by Eurocodes, is illustrated in Fig. 5 where pedix, “c” is associated to confined properties of concrete. The presence of stirrups modifies strength and ductility of concrete as follows:

Table 1 Mechanical properties of PCs/FRCs (Eurocode 8)

Mechanical property	Plain concrete		Fibre reinforced concrete		
	C25/30	C40/50	FRC25/30	FRC50/60	FRC80/95
R_{ck} (MPa)	30	50	30	60	95
f_{ck} (MPa)	25	40	25	50	80
f_{cd} (MPa)	14.17	22.67	14.17	28.33	45.33
E_{cm} (MPa)	31,476	35,220	31,476	37,278	42,244
f_{ctk} (MPa)	–	–	1.80	2.9	3.20
f_{ctd} (MPa)	–	–	1.20	1.9	2.13
ϵ_{tu}	–	–	3%	3%	3%

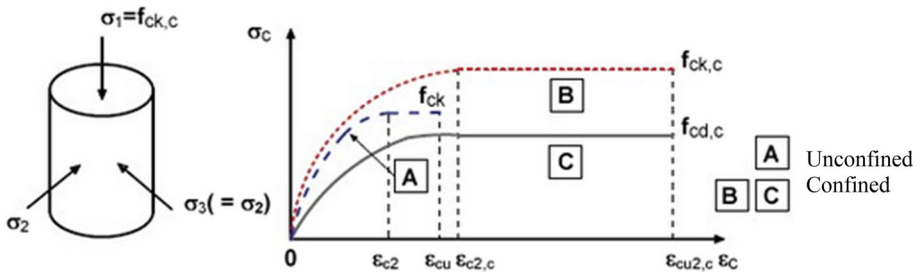


Fig. 5 Confinement effect due to stirrups on concrete behaviour

$$\begin{aligned}
 f_{ck,c} &= f_{ck}(1 + 5\sigma_2/f_{ck}) \quad \text{if } \sigma_2 \leq 0.05f_{ck} \\
 f_{ck,c} &= f_{ck}(1.125 + 2.5\sigma_2/f_{ck}) \quad \text{if } \sigma_2 \geq 0.05f_{ck} \\
 \epsilon_{c2,c} &= \epsilon_{c2}(f_{ck,c}/f_{ck})^2 \\
 \epsilon_{cu,c} &= \epsilon_{cu} + 0.2\sigma_2/f_{ck}
 \end{aligned}
 \tag{1}$$

σ_2 is the lateral effective pressure developed by stirrups and can be determined as $\sigma_2/f_{ck} = 0.5 \alpha \omega_{wd} = 0.5 a_n a_s (V_{stirrups}/V_{confined}) (f_{ywd}/f_{cd})$, where a_n and a_s are respectively the confinement efficiency factors in the section and along the element, assumed as equal as 1 in absence of specific information. It can be noticed that a different confinement effect is obtained for inelastic and elastic regions of frames since stirrups have different spacing. In fact, in inelastic and elastic regions stirrups are spaced respectively 120 and 180 mm. Hence, the choice among the models proposed by the software library ended with: Kent and Park constitutive model (1971) as modified by Scott et al. (1982) for unconfined plain concrete, Nagoya Highway Corporation model for confined plain concrete and for fibre reinforced concrete. The first one is described by a parabolic-softening curve in compression, while the second one is a parable-rectangle curve in compression and is bilinear in tension. The ultimate tensile stress of FRCs is set to zero due to the numerical implementation of the model. Therefore, the contribution of fibres to the strength of the structures under examination should be considered conservative although it has been assessed that in no case the ultimate tensile strain of 2%, suggested by Model Code 2010 (FIP Model Code 2010), has been exceeded in the analyses. Figure 6 illustrates the above-mentioned constitutive models.

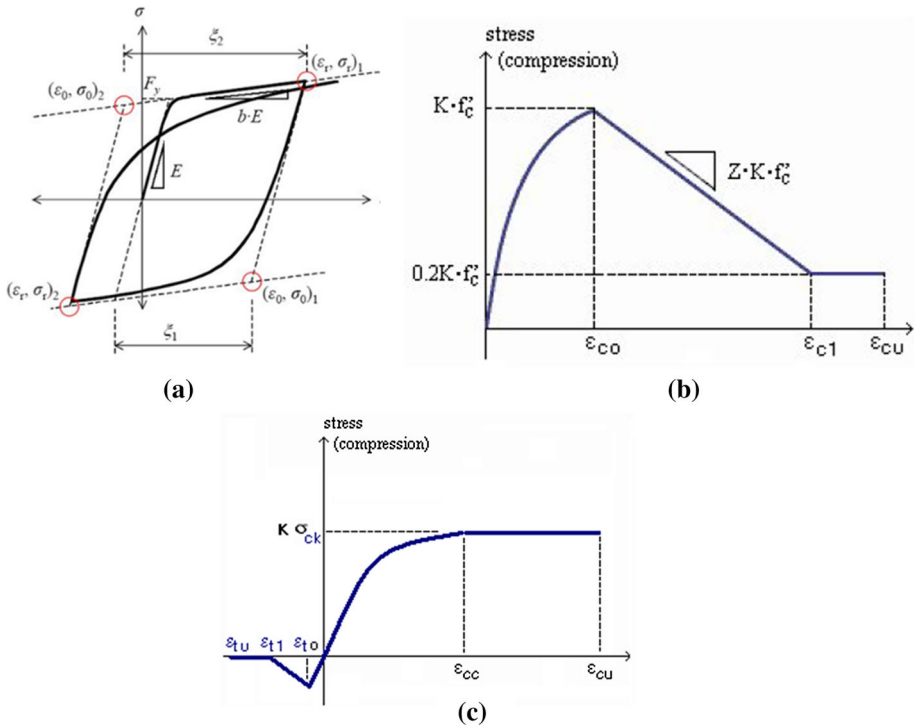


Fig. 6 Material constitutive models: **a** Menegotto and Pinto’s model for steel; **b** Kent and Park’s model for plain concrete; and **c** Nagoya Highway Corporation model for HPFRC

4 Fibre sections and M–N interaction envelopes

The distributed plasticity allows improved accuracy on the nonlinear response of structures if compared to concentrated plasticity, where nonlinearity belongs to an assigned number of cross-sections. The member stress–strain state is obtained by integration of the non-linear uniaxial response of single fibres that form the cross-section. To the aims of the present paper, force-based elements are conveniently adopted, where shape functions are oriented to the exact determination of forces in the elements (Spacone et al. 1996). Each section is discretized in about 100 fibres (10 × 10), distinguishing confined and unconfined regions and steel reinforcements. Figure 7 reports the fibre section discretization assigned to columns and beams, including 100 fibres, ten per side.

Figure 8 shows the M–N interaction envelopes for a 400 × 400 mm square section (1% of reinforcing steel; 40/50 and 80/95 class plain and fibre-reinforced concretes). Two curves are depicted referring to the envelopes obtained by computing the RC and FRC sections. The difference between RC and FRC sections in Fig. 8 is associated to the contribution offered to tensile force by the residual strength of FRCs, if taken into consideration.

The results show that the introduction of fibres affects the ultimate strength of RC members with an appreciable, but small, increment (according to the longitudinal reinforcement ratio). At the same time, the numerical tests on cantilever beams, which were run to calibrate the numerical model, exhibit an enhanced ductility when FRC is used, as

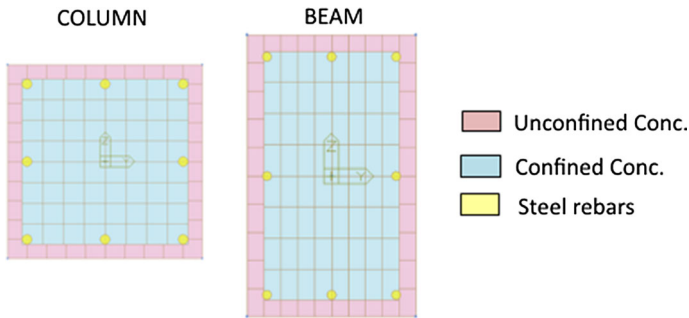


Fig. 7 Fibre section discretization for beams and columns

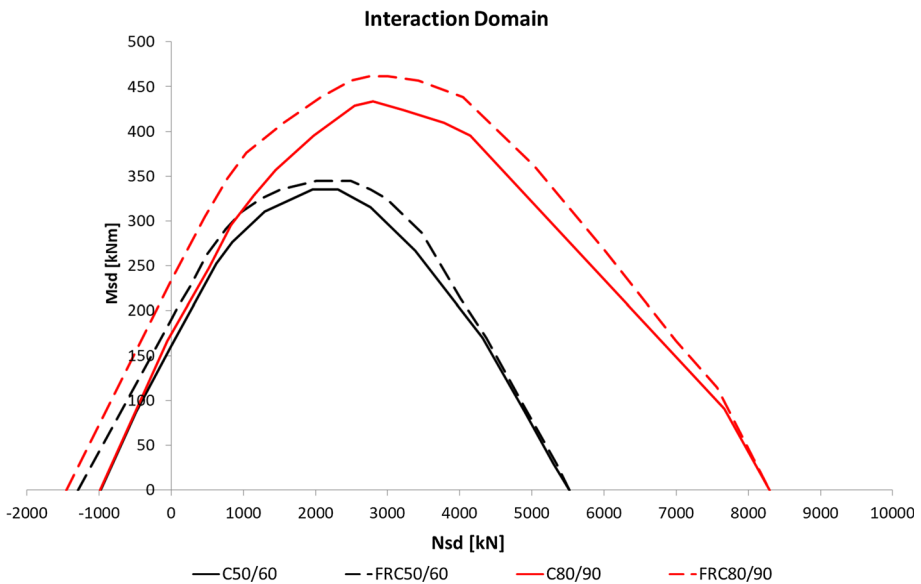


Fig. 8 M–N interaction envelopes

shown in Fig. 9. In bending, the raise of a distribution of tensile stress, along the section height of the concrete frame member engenders—by internal equilibrium—an increment of the resultant compression force. Therefore, an increased resisting moment arises at a sectional level, especially when HPFRCs are used.

5 Assessment of capacity design

According to capacity design, the condition *weak-beam strong-column* has been assessed for all frames in order to determine if the failure mechanisms of the investigated structures occur as desired by the modern provisions of seismic design. For the sake of brevity, a simplified assessment is reported for a representative condition in this paper. Taking into account a plain concrete grade C25/30, all beams have a resisting moment of 139.2 kNm. The weakest column has size 40×40 cm and $8\Phi 20$, three bars per side. In order to have a

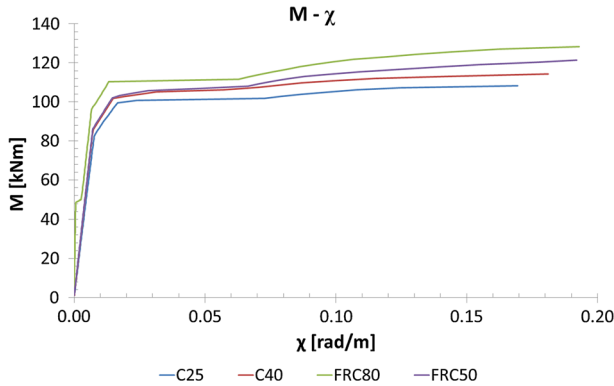


Fig. 9 Moment–curvature relationships

general validity for all of the investigated frames, the presence of a vertical axial load in columns has been neglected. That is on the safe side according to the directions provided by Eurocode 8 in section 4.4.2.3. Indeed, the actual resisting moment is always greater than the assumed value, as the axial load is always included between zero value and the value corresponding to the maximum resisting moment. Therefore, assuming a null axial load, columns have a resisting moment greater or equal to 168.4 kNm. The equation provided by Italian Standards for low ductility class building is therefore assessed:

$$\sum M_{columns} \geq 1.1 \sum M_{beams} \tag{2}$$

6 Analysis and results

6.1 Pushover analysis

A pushover analysis with displacement control is performed for the set of frames previously described. Both linear triangular and uniform (mass proportional) load profiles are adopted and computed according to paragraph 7.3.4.1 of NTC08 and paragraph 4.3.3.4.2.2 of EC8, with respectively Group 1 and Group 2 distribution types. The two load profiles are respectively proportional to the deformed shape of the first mode and to the masses of floors.

The results of the analysis consist of a wide database of pushover curves (where the control point is the roof centroid), moment versus curvature diagrams of the lateral base column, and deformed shapes at the end of the analysis. All the pushover curves are reduced to a bi-linear curve of a SDOF system. Therefore, behaviour factors can be computed and analysed by means of statistical analysis.

Only the most representative results are presented in the following figures, in order to draw general trends. The title of lines represented in most of the figures below follows a simple rule. The first part, e.g. 2 × 2, identifies the frame geometry and a letter, F or R, which distinguishes the joint modelling techniques between rigid link and fibre element, follows it. Then, a letter L or C identifies the load profile, whether linear or constant (uniform). If perfect in-plane stiffness of floors is considered than the letter D, standing for rigid diaphragm, precedes F or R. Finally, the combination of materials is reported (i.e.

FRC50/RC25). Therefore, for example, the code $2 \times 4\text{-F-L-FRC50/RC25}$ univocally identifies the two-bay four-storey frame, linear load profile, fibre-based joint, with FRC50 and RC25 respectively for inelastic and elastic regions.

Figure 10 shows the pushover curves obtained for the frames 2×8 and 4×4 , respectively, according to different load profiles and different modelling techniques. Firstly, the modelling technique of the joint does not play any role in the study of the global behaviour. In fact, there are no significant variations when comparing the results obtained by modelling the nodal zones as rigid end-sections or rather as deformable elements with distributed plasticity. Indeed, the load profile has an influence on the response of frames, as it is commonly acknowledged in the scientific community [e.g. Gupta and Kunnath (2000), Mwafy and Elnashai (2001)]. When applying a uniform load profile, pushover curves show greater values of total base shear and lower values of ultimate displacements compared to the pushover curves obtained using linear load profiles.

Figure 11 illustrates push-over curves for all material combinations in frame 4×4 , with uniform (a) and linear (b) loadings, and if perfect in-plane stiffness of floors is assumed (c). Figure 12 illustrates the results obtained for frames 4×2 and 4×8 . Therefore, it is possible to compare the behaviour of the assumed frames while evaluating the effects of all the investigated variables.

A general increment of total shear capacity is assessed for mixed FRC/RC frames compared to the reference RC frames. The increment is proportional to the number of bays—simply due to a greater number of columns—and to building height, due to the beneficial effect of axial load in the bending capacity of columns. The ultimate top displacements increase with the height of the building but decrease for a larger number of bays, due to increased lateral stiffness. The pushover curves related to material combinations FRC80/RC40 and FRC80/RC25, display sometimes a softening behaviour. Furthermore, in such cases it is observed that the failure of the first element moves from the inelastic regions of columns towards the elastic central part, when increasing the number of storeys. If such undesirable situation occurs, then the mechanical properties of FRC80 are not fully exploited, due to excessive difference in the mechanical performances of materials. Figure 13 shows the moment versus curvature diagrams for the lateral base column of frame 4×8 with all material combinations. In the case of material combination FRC80/RC25 the base section of the column is not able to exploit its deformation capacity since the failure occurs in the elastic region where RC25 is used. When the rigid diaphragm

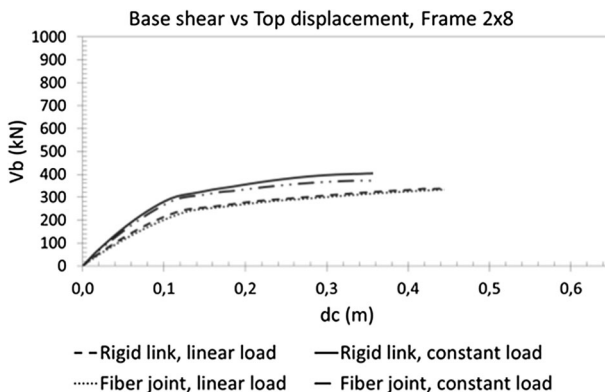


Fig. 10 Pushover curves for frames 2×8

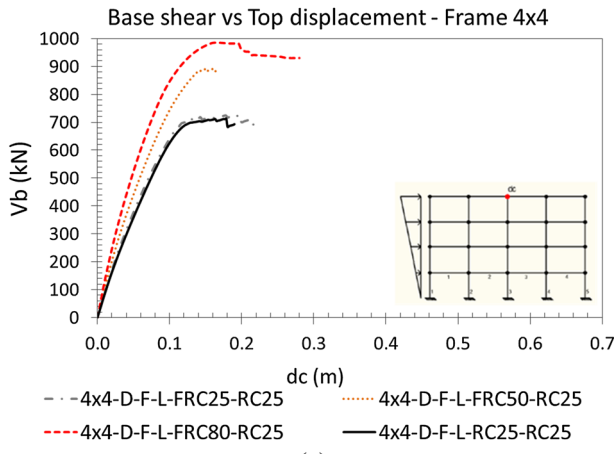
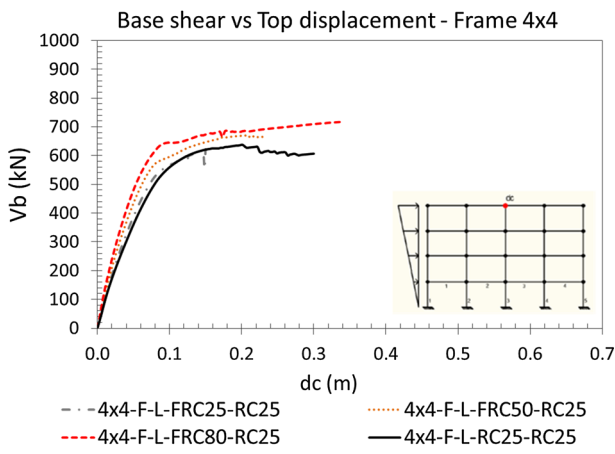
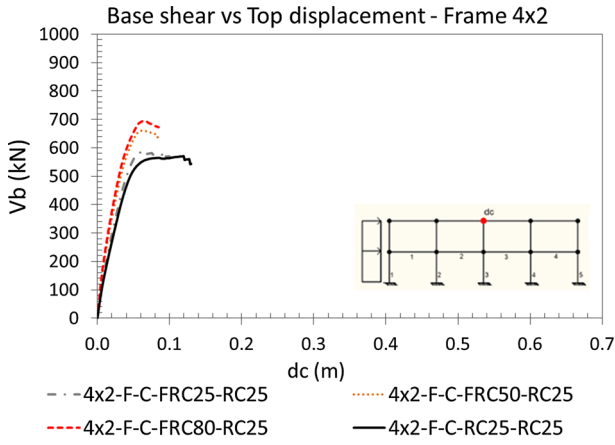


Fig. 11 Pushover curves for frames 4×4 : **a** uniform load; **b** linear load; **c** floor in-plane perfect stiffness

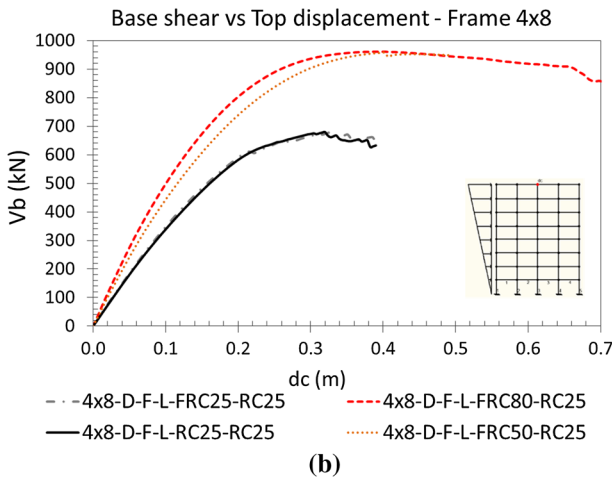
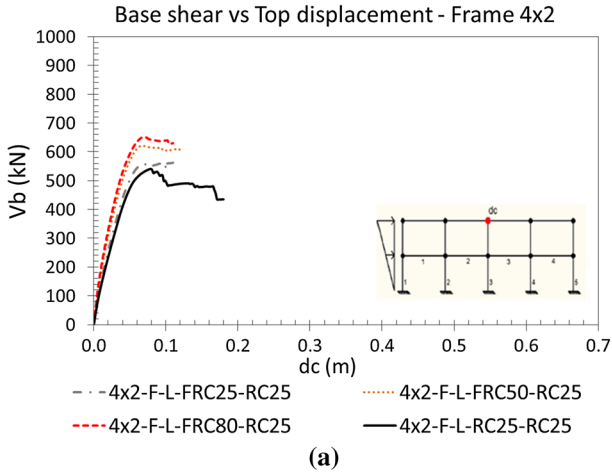


Fig. 12 Pushover curves for linear load: **a** frame 4×2 ; **b** frame 4×8

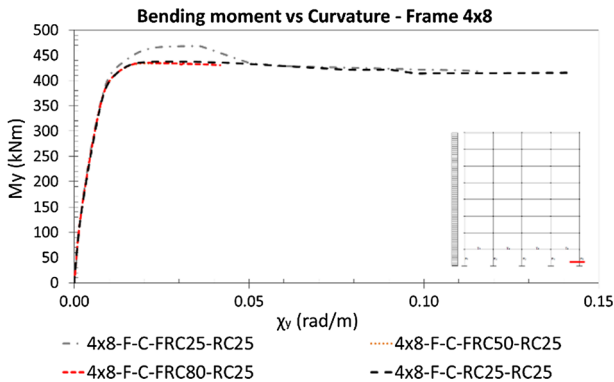


Fig. 13 Bending moment versus curvature in lateral base columns, frame 4×8

constraint is used to account for perfect in-plane stiffness of floors, frames develop a greater total shear capacity, taking full advantage of the properties of FRCs. Assuming stiff floors brings in a uniform demand of lateral displacement along the columns, thus at the end of the analysis the collapsed element undergoes smaller rotations than under the assumption of deformable floors. Therefore, the floor constraint has a strong influence on the behaviour of the frames, which becomes more significant as the number of the storeys increases. The increment of capacity is associated with a reduced ultimate top displacement for 2-storey frames while in higher frames the constraint implies larger ultimate displacements.

The results presented so far allow making a further comment. All the frames designed with a combination of FRC50/RC25 materials have a better performance than the reference frames, while the pushover curves exhibit a hardening behaviour. Coupling cementitious materials with major differences in terms of strength, elastic modulus, shrinkage, creep and intrinsic ductility may cause serious problems.

Given the pushover curve, the bilinear SDOF equivalent curve—obtained in accordance with NTC08—is univocally determined. On the contrary, EC8 allows making a choice between a perfectly plastic or a hardening behaviour, providing no indications on the elastic stiffness. That is the main difference between the two procedures. In the present paper, the Italian Building Code is adopted as reference for the determination of behaviour factors.

6.2 Behaviour factor

Behaviour factors can be determined by pushover analysis adopting the simplified approach commonly followed by the most recent design codes and guidelines, such as Eurocode 8. The value of behaviour factor is obtained as follows:

$$R = R_{\mu}\Omega \quad (3)$$

where Ω is the so-called over strength factor, obtained as the ratio between the two values of total base shear corresponding respectively to the start of the collapse mechanism and the formation of the first plastic hinge. R_{μ} is the ductility factor that depends on intrinsic ductility, damping and on first natural frequency of the structure. The estimation of R_{μ} can be based on several analytical formulations proposed by Newmark and Hall (1982), Krawinkler and Nassar (1992), Fajfar (2000) and Priestley and Paulay (1992). The formulas provide results that are in very good agreement, as expected, apart for Krawinkler and Nasser formula that is quite conservative. The equations proposed by Newmark and Hall, Fajfar and Priestley lead respectively to the same values of behaviour factor when $T > 1.5 T_c \geq 0.5$ s. In Eurocodes and Italian Standards the behaviour factor is equivalently labelled as q . Table 2 reports the values of behaviour factor computed according to the four methods for all frames, with fibre joints and uniform lateral loading. However, in order to be coherent, the results presented so far are obtained according to the formula proposed by Fajfar (2000), which produces the highest values. For each of the analysed frames, the failure mechanism is identified and the formation of the first plastic hinge is detected. Generally, it occurs by yielding of steel reinforcements or, if concrete has a low grade, by the reaching of strain at maximum strength. Figure 14 shows an example for the determination of the step of first plastic hinge formation. The determination of the variables introduced is obtained by means of the bi-linearization of pushover curve reduced to Single

Table 2 Behaviour factors for all frames, fibre joints and uniform loading, computed according to Newmark and Hall (N&H), Krawinkler and Nassar (K&N), Fajfar (F) and Priestley (P)

Fibre joint uniform load		Behaviour factor			
		N&H	K&N	F	P
2 × 2	FRC25–RC25	3.20	2.33	3.38	2.74
	FRC50–RC25	3.19	2.49	3.39	2.71
	FRC80–RC25	3.10	2.27	3.14	2.56
	FRC80–RC40	3.08	2.30	3.09	2.51
	RC25–RC25	3.86	2.72	4.37	3.42
	RC40–RC40	3.57	2.48	3.77	3.01
2 × 4	FRC25–RC25	4.40	3.39	6.45	5.61
	FRC50–RC25	4.69	3.92	7.45	6.23
	FRC80–RC25	4.94	4.16	8.15	6.63
	FRC80–RC40	5.58	5.47	10.76	8.39
	RC25–RC25	4.92	3.38	7.22	6.28
	RC40–RC40	5.32	3.88	8.43	6.97
2 × 8	FRC25–RC25	6.50	3.52	6.50	6.50
	FRC50–RC25	4.71	3.12	4.71	4.71
	FRC80–RC25	5.66	3.80	5.66	5.66
	FRC80–RC40	5.72	3.83	5.72	5.72
	RC25–RC25	5.39	2.84	5.39	5.39
	RC40–RC40	5.44	3.14	5.44	5.44
4 × 2	FRC25–RC25	3.11	2.38	3.39	2.73
	FRC50–RC25	2.48	1.94	2.47	2.09
	FRC80–RC25	2.45	1.96	2.42	2.04
	FRC80–RC40	2.55	2.00	2.50	2.10
	RC25–RC25	3.39	2.40	3.71	2.98
	RC40–RC40	3.02	2.08	3.07	2.55
4 × 4	FRC25–RC25	5.65	2.87	5.65	5.06
	FRC50–RC25	3.83	3.02	5.33	4.62
	FRC80–RC25	4.22	3.37	6.22	5.24
	FRC80–RC40	4.86	4.32	8.18	6.62
	RC25–RC25	7.74	3.64	7.74	6.84
	RC40–RC40	4.91	3.29	7.13	6.10
4 × 8	FRC25–RC25	4.93	2.66	4.93	4.93
	FRC50–RC25	4.51	3.01	4.51	4.51
	FRC80–RC25	5.10	3.51	5.10	5.10
	FRC80–RC40	5.67	3.83	5.67	5.67
	RC25–RC25	4.84	2.41	4.84	4.84
	RC40–RC40	5.08	2.70	5.08	5.08

Degree Of Freedom curve. Figure 15 shows a pushover curve, its corresponding SDOF curve and the bilinear curve obtained according to NTC08.

Figure 16 illustrates the mean values of behaviour factors and corresponding standard deviations for the investigated frames, distinguished by categories: respectively

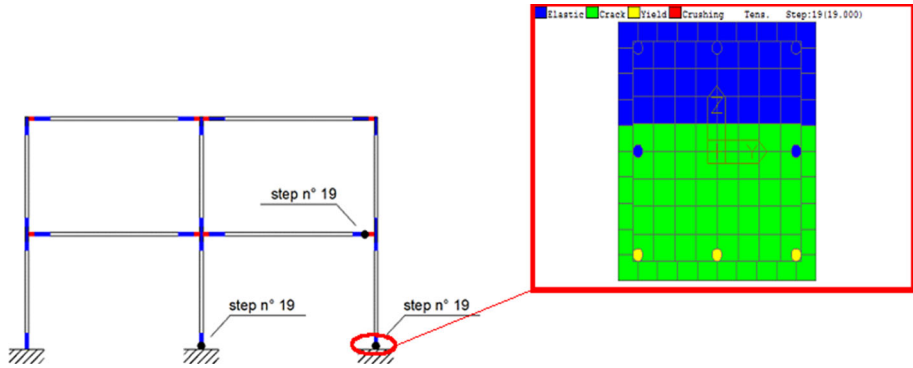


Fig. 14 Example of identification of the step at first plastic hinge formation

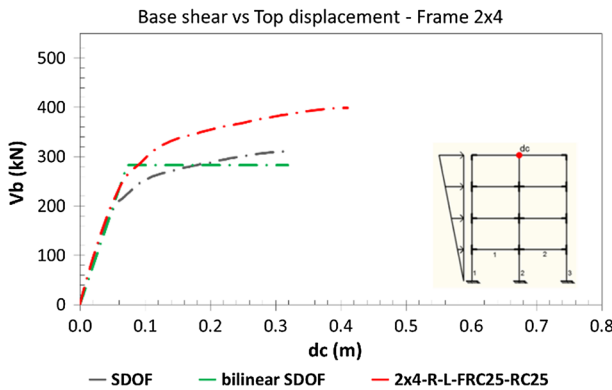


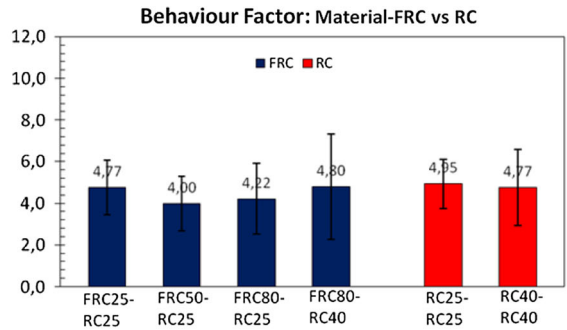
Fig. 15 Determination of SDOF curve and corresponding bilinear curve

(a) geometry, (b) material combinations, (c) lateral load profile and (d) in-plane stiffness constraint.

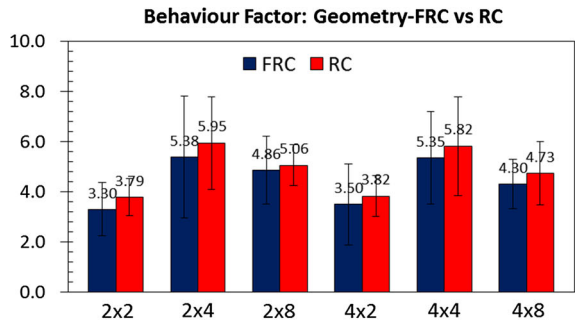
The highest values of behaviour factor are obtained for 4-floor buildings, which always show a global failure mechanism. The analysed 8-floor buildings may be unable to fully exploit their global ductility, as in some cases very few plastic hinges formed in the upper two or three floors without reaching their ultimate rotations. Generally, the values of behaviour factors decrease as the number of spans increases. When FRC is used in joint regions, there is a decrement of the values of behaviour factor. Such difference can be explained by the stiffening effect due to the use of a higher-grade material compared to the reference concrete. Joint modelling technique and lateral load profile do not influence the values of behaviour factor at all, while perfect in-plane stiffness of floors is the most influencing variable on behaviour factor. If diaphragm constraint is used, then the mean behaviour factor is reduced by 30% independently from the use of FRC in joint regions.

According to the simplified procedure suggested by NTC08, all the investigated frames should have a behaviour factor as equal as 3.9. That is the value for regular multi-storey multi-span frames, in low ductility class CDB. The outcomes of pushover analyses show comparable values of behaviour factor for both ordinary concrete and fibre reinforced concrete frames. Only 2-storey frames may be unable to develop the value of behaviour

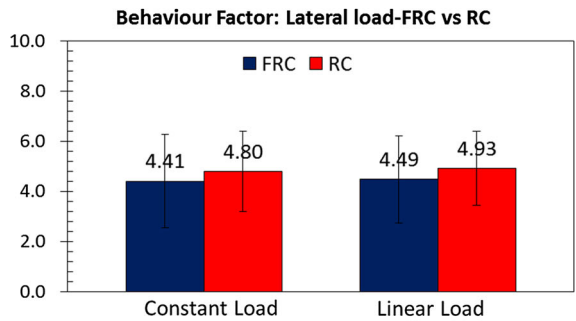
Fig. 16 Behaviour factor R: **a** material combination; **b** geometry; **c** lateral load; **d** in-plane stiffness



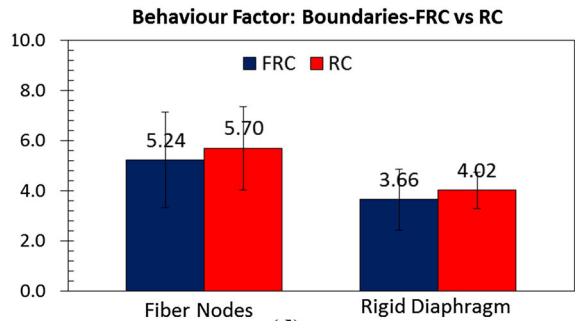
(a)



(b)



(c)



(d)

factor suggested by NTC08 due to inadequate dissipation capacity. However, that is not surprising, as the number of possible plastic hinges is very small.

Tukey Range TEST confirms the considerations provided above. Figure 17 reports the outcomes of such test. Tukey test identifies which of the investigated variables cause a variance in the analysed data (p value > 0.1). If p -value is lower than 0.1, then the variable is not influencing the variance. In particular, the Tukey test returns that lateral loading profile (linear or constant) and joint modelling technique (rigid links or fibre joints) do not influence the variance at all. On the contrary, the number of storeys is the most influential variable on the value of behaviour factor. Tukey test showed that 80% of the variance is justified by the investigated variable, while the remaining 20% might be depending on incoherent results; this is the case of some of the 8-storey frames where undesired collapse mechanism occurs.

6.3 Incremental dynamic analysis

Incremental dynamic analysis involves an extensive number of time-history analyses based on accelerograms scaled by the Scale Factor (SF), which has been linearly varied until frame failed. IDA analysis returns discrete points in terms of total base shear (V) and top displacement (d_c), while pushover analysis provides a continuous relationship. As during a dynamic analysis the maximum values of shear and top displacement do not occur at the same instant, it is useful to draw diagrams in terms of both $V(d_{c,max})$ versus $d_{c,max}$ and V_{max} versus $d_{c,max}$. Figure 18 shows the results of analysis for frames 2×2 with material combinations RC25-RC25 and FRC80-RC25, as the most representative cases. Figure 18a clearly illustrates the good agreement between pushover curves and discrete points obtained with dynamic analysis. These points, in fact, are associated to balanced and congruent schemes. Figure 18b, instead, shows the maximum values of base shear obtained during dynamic analysis, which might be much greater than the values of maximum shear determined by means of pushover analysis. Both diagrams also demonstrate, as well, that in some cases the maximum values of top displacement obtained with IDA analysis may be higher than those provided by pushover analysis. In a few cases, it is the opposite. This is probably due to the difference in the pattern of congruent displacements associated to static and dynamic nonlinear analyses. Notice that in Fig. 18 the maximum displacement and the maximum total base shear do not occur at the same time. The increase in base shear and top displacement values is more pronounced in mixed RC/FRC frames compared to

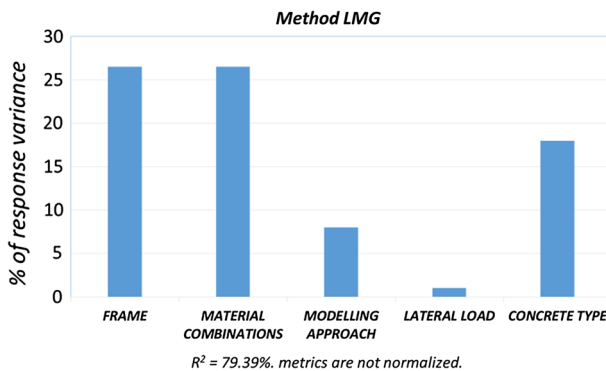


Fig. 17 Outcomes of Tukey test

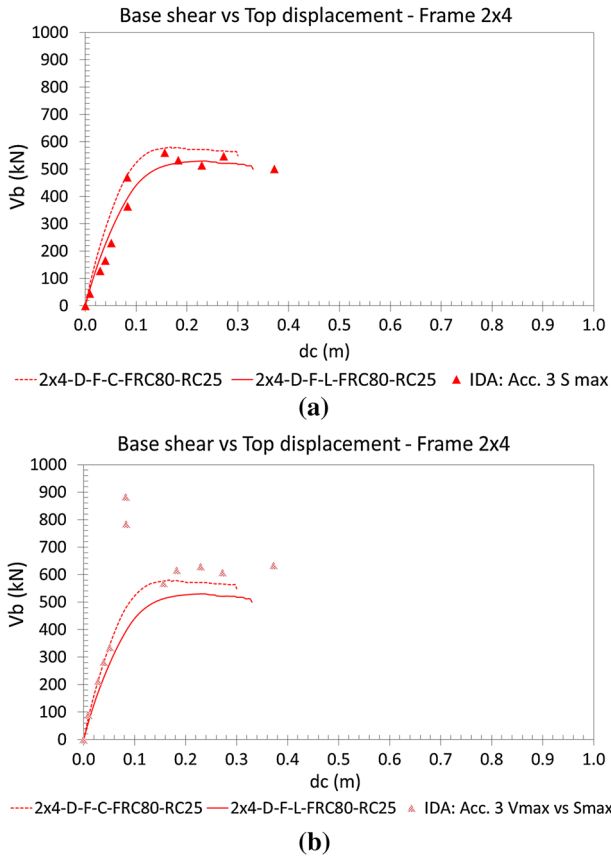


Fig. 18 Capacity curves for accelerogram #3, frame 2×4 , FRC50–RC25: **a** $V(d_{c,max})$ versus $d_{c,max}$; **b** V_{max} versus $d_{c,max}$

ordinary frames. Indeed, it is most significant for the tallest structures. In exceptional cases, maximum shear and displacement values can be even doubled. Therefore, the assessment of shear capacity based on push-over analysis should be carried out by adopting a partial safety factor while, at the same time, the values of the behaviour factors obtained in the preceding paragraph shall be considered to be conservative. Otherwise, the total base shear demand due to seismic events can be dangerously underestimated by pushover analysis.

Table 3 reports a quantitative comparison between the results obtained performing both pushover and incremental dynamic analysis, for two-bay frames.

6.4 Shear capacity of frames

All analyses are based on the nonlinear distributed plasticity theory, considering only flexural failure mechanisms for members. Therefore, shear failures are excluded by assumption. In fact, brittle failures are prevented by design criteria adopted for the design of frames, according to NTC08 and EC8. However, the assessment of shear capacity has been carried out element by element, frame by frame. Table 4 reports the total base shear capacity of the two-bay frames investigated in the numerical analysis. The shear resistance

Table 3 Quantitative comparison between total shear and top displacement demands for two-bay frames, estimated with pushover and IDA

Materials	IDA		Pushover (uniform)		Pushover (linear)	
	V_{\max} (kN)	$D_{c,\max}$ (m)	V_{\max} (kN)	$d_{c,\max}$ (m)	V_{\max} (kN)	$D_{c,\max}$ (m)
<i>Frame 2 × 2</i>						
RC25/RC25	496	0.16	340	0.13	337	0.19
FRC50/RC25	509	0.15	402	0.08	390	0.10
FRC80/RC25	557	0.33	427	0.08	417	0.12
<i>Frame 2 × 4</i>						
RC25/RC25	592	0.33	427	0.21	384	0.25
FRC50/RC25	508	0.15	511	0.16	457	0.15
FRC80/RC25	687	0.43	427	0.08	417	0.12
<i>Frame 2 × 8</i>						
RC25/RC25	669	0.79	425	0.36	349	0.43
FRC50/RC25	866	0.90	504	0.27	416	0.45
FRC80/RC25	1056	1.13	561	0.28	488	0.50

Table 4 Shear capacity of single columns and two-bay frames

Column shear capacity		Total base shear capacity	
Size 40 × 40	341 kN	Frame 2 × 2	1023 kN
Size 45 × 45	387 kN	Frame 2 × 4	1161 kN
Size 50 × 50	483 kN	Frame 2 × 8	1449 kN

of columns is determined considering the real size of base columns and stirrup spacing (12 cm in inelastic zones), while the contribution of fibres to shear strength is neglected. Therefore, the incremented total base shear demand does not imply any shear failure and capacity design rules are still satisfied. The capacity curves plotted so far are fully realistic.

6.5 Fragility curves

For the evaluation of the seismic vulnerability, fragility curves can be drawn. Fragility curves provide the average value of the damage in a construction as a function of a seismic intensity measure (IM) parameter, or the probability of exceeding a certain level of damage depending on the input. In the present paper, IM parameter is represented by a scale factor (SF) multiplied by the peak ground acceleration (PGA). In such a way, the IM parameter depends on two independent variables that account for site hazard and frame response respectively. Two different methods are discussed according to the approach of the maximum likelihood presented by Baker (2015) and hereafter referred to as Incremental Dynamic Analysis (IDA) and MSA (Multiple Stripe Analysis). In the case of incremental dynamic analysis, the fragility curve is a classical curve of cumulative distribution based on the statistics of failures, which might be truncated at a fixed IM level. The multiple stripe analysis method takes into account a binomial probability function that includes the probability of both failures and non-failures associated with predetermined IM values. As a

direct consequence, while IDA analysis can only rely on the information related to failure for the given seven accelerograms, MSA can count on information about the performance of frames for a number of IM levels. MSA and truncated IDA are extremely convenient when an efficient fragility curve is required based on a number of accelerograms associated with different IM levels, without having knowledge of what is the IM value that implies a 100% of failure probability. However, that is not the case under examination. In fact, for any accelerogram the value of SF associated with a 100% probability of collapse is determined with the aim to compare the results obtained with pushover and IDA analysis.

Figure 19 shows the fragility curves based on the given 7 accelerograms for frames 2×2 with material combinations of type RC25-RC25 and FRC80-RC25. It is observed that the difference between the fragility curves obtained with the two methods is contained for the frames under investigation, but in some cases important differences may arise. Figure 19 shows that mixed frames have a lower probability of collapse for a given value of IM, as the grade of FRC used in dissipative zone increases. The MSA method has produced more precautionary curves for the frames under consideration. Figure 20 shows fragility curves for frame 2×4 and 2×8 , computed according to IDA method. The figures prove that the probability of collapse decreases with increasing number of storeys (height), confirming the expectation that earthquakes may have a lower impact on higher buildings, whose higher first mode periods are associated to a lower value of pseudo-acceleration in the design spectrum.

6.6 Failure mechanisms

For each frame under investigation, all sections are monitored in order to identify the collapse mechanisms. Figure 21 shows the single case of frame 2×4 , FRC50-RC25. In the representation, the empty blank circles indicate reinforcement yielding, the partially black circles indicate concrete cover crush, while the black dots indicate the failure of sections, where ultimate material strains are achieved.

In all cases, a global collapse mechanism arises, with formation and rupture of plastic hinges, formed at beam-ends first and then at column bases. Figure 21 clearly shows how IDA analysis achieves a more widespread plasticization of structural members, including the height of columns. Note that during IDA analysis much larger lateral displacements are

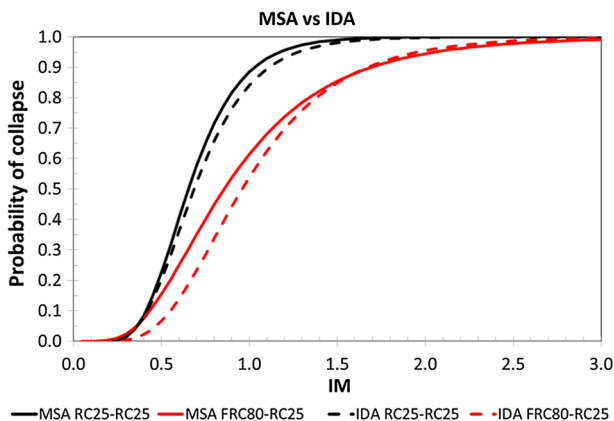


Fig. 19 Fragility curves for frames 2×2 ; comparison between MSA and IDA

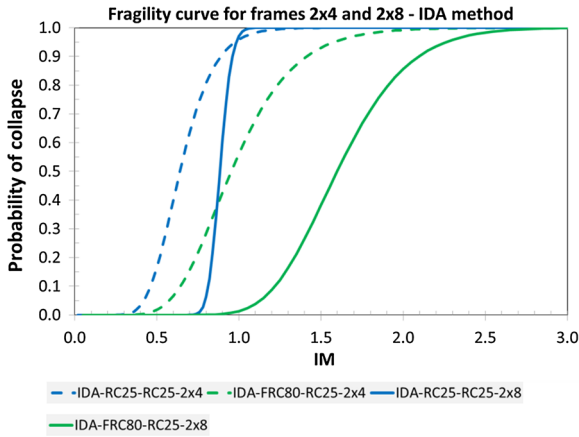


Fig. 20 Fragility curves for frames 2×4 and 2×8 —IDA

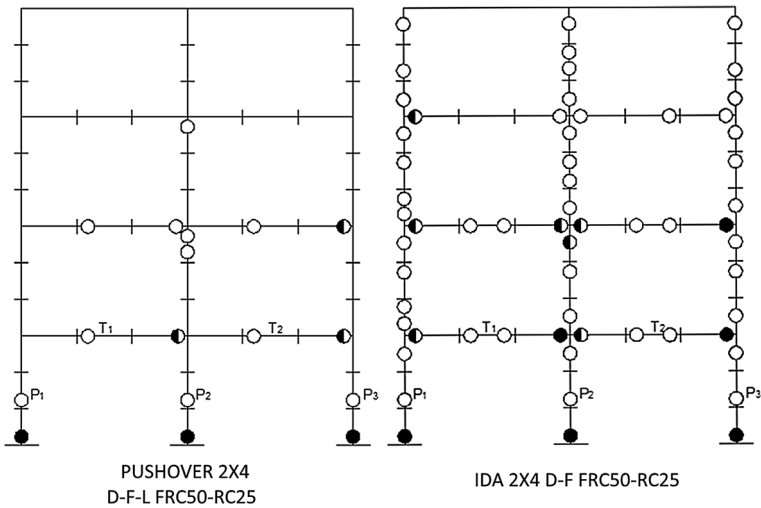


Fig. 21 Failure mechanisms, frame 2×4 , FRC50–RC25: (left) Pushover; (right) IDA

achieved for the case represented in the figure, implying larger distribution of plasticity. In some of the frames with use of HPFRC in association to ordinary plain concrete, an undesirable collapse mechanism may arise according to the results of pushover analysis. The mechanism is still global, yet plastic hinges form in the central part of the base columns, about at one-third of the height, where inelastic behaviour is not expected. Therefore, again, mixed RC/FRC frames need to couple plain and fibre reinforced concrete with similar grades.

7 Conclusions

The study of the mechanical performance of RC/FRC frames is one of the topics at the forefront of today's research activities in the structural domain, which is mainly devoted to experimental behaviour of columns, beam-column joints and frames subjected to cyclic actions. Beyond any doubt, the performance of FRC members, even devoid of transverse reinforcement, positively affects tensile, shear and bending behaviours.

The purpose of this work is to investigate the use of fibre-reinforced materials in the critical regions of concrete frames subjected to seismic loads, where a high dissipation ability is required. A numerical investigation focused on the global behaviour of earthquake-resistant RC plane frames with FRC materials in the joint regions was presented and discussed. Static and dynamic non-linear analyses were performed, based on a diffused plasticity model with fibre sections. Investigations on a number of variables such as frame geometry, FRC/RC material grade combinations, lateral load profile, joint modelling technique and floor in-plane constraint are carried out. Frames with FRC in joints prove to have better performances than reference RC frames. In fact, in FRC frames the total base shear capacity is higher than in reference frames, while the behaviour factor is not affected as much and the collapse probability is increased. Therefore, for a given geometry, adopting fibre-reinforced materials in the joints brings in not only a higher lateral stiffness, but also a higher global capacity, leading to reduced lateral displacements in case of non-destructive earthquakes (Serviceability Limit State). However, when the FRC material has a grade far from that of the plain concrete used in elastic regions, failures may occur in the plain concrete central part of columns, in that case the properties of the fibrous material are not fully exploited. In such cases, at construction joints FRC sections may remain elastic and no yielding occurs in the reinforcement. Especially for FRCs, IDA analysis showed improved total base shear demand and ultimate top displacements. For the investigated frames, IDA analysis provides more accurate results than pushover analysis, since non-linear effects are better caught. Collapse probability decreases with the number of storeys and when FRC is used in critical regions. Furthermore, the comparison between fragility curves determined by means of Multiple Stripes Analysis and Incremental Dynamic Analysis based on maximum likelihood show that MSA produces curves that are more conservative.

Other than the behaviour of mixed RC/FRC frames, the analysis has led to interesting additional conclusions. Firstly, the way in which the joints are modelled (either as rigid end-sections or as deformable elements) is almost irrelevant in terms of global behaviour of frames. The load profile influences the frame response in terms of lateral stiffness, maximum resistance and lateral displacements at failure. Indeed, the load profile implies different base shear versus displacement curves, but not different behaviour factors. In particular, uniform load profiles lead to higher base shear but lower ultimate displacement compared to linear load profiles. The constraint offered by *stiff floors* plays the most influential role that increases with the height of the frames. The constraint allows the properties of fibre-reinforced concrete to be fully exploited, especially in the sections at the base of the columns. Consequently, pushover curves show a stiffer and stronger behaviour. Rigid diaphragm constraint influences the behaviour factor as well, independently from the use of FRC materials. As a general trend, the behaviour factor tends to decrease. However, for higher frames the ultimate displacement can significantly increase.

In order to validate or re-discuss the results of the present study and to solve possible problems related to concrete technology in the field, further experimental studies will be necessary.

References

- Baker JW (2015) Efficient analytical fragility function fitting using dynamic structural analysis. *Earthq Spectra* 31(1):579–599
- Bayasi Z, Gebman M (2002) Reduction of lateral reinforcement in seismic beam–column connection via application of steel fibres. *ACI Struct J* 99(6):772–780
- Di Prisco M, Plizzari GA, Vandewalle L (2009) Fibre reinforced concrete: new design perspectives. *Mater Struct* 42(9):1261–1281
- EN:1991-1-1:2002 Eurocode 1: general actions. densities, self-weight, imposed loads for buildings
- EN:1998-1:2004 Eurocode 8: design of structures for earthquake resistance. Part 1: General rules, seismic actions and rules for buildings
- Fajfar P (2000) A nonlinear analysis method for performance-based seismic design. *Earthq Spectra* 16(3):573–592
- FEMA-356 (2000) NEHRP guidelines for the seismic rehabilitation of buildings
- Filiatrault A, Pineau S, Houde J (1995) Seismic behaviour of steel-fibre reinforced concrete interior beam–column joints. *ACI Struct J* 92(5):543–552
- Filippou FC, Popov EP, Bertero VV (1983) Effects of bond deterioration on hysteretic behavior of reinforced concrete joints. Report No. UCB/EERC-83/19
- FIP MODEL CODE (2010) In: 37th conference on our world in concrete & structures
- Fischer G, Li VC (2002a) Effect of matrix ductility on de-formation behavior of steel-reinforced ECC flexural members under reversed cyclic loading conditions. *ACI Struct J* 99(6):781–790
- Fischer G, Li VC (2002b) Influence of matrix ductility on tension-stiffening behavior of steel reinforced engineered cementitious composites (ECC). *ACI Struct J* 99(1):104–111
- Fischer G, Li VC (2003) Deformation behavior of fibre-reinforced polymer reinforced engineered cementitious composite (ECC) flexural members under reversed cyclic loading conditions. *ACI Struct J* 100(1):25–35
- Gupta B, Kunnath SK (2000) Adaptive spectra-based pushover procedure for seismic evaluation of structures. *Earthq Spectra* 16(2):367–391
- Henager CH (1977) Steel fibrous-ductile concrete joint for seismic-resistant structures. Publication, *ACI Spec*, p 53
- Italian Building Code (2008) DM 14.01. 2008: Norme tecniche per le costruzioni. Italian Ministry of Infrastructures and Transportation, Rome, Italy
- Jiuru T, Chaobin H, Kaijian Y, Yongcheng Y (1992) Seismic behavior and shear strength of framed joint using steel-fibre reinforced concrete. *J Struct Eng* 118(2):341–358
- Kent DC, Park R (1971) Flexural Members with Confined Concrete. *J Struct Division* 97(7):1969–1990
- Krawinkler H, Nassar AA (1992) Seismic design based on ductility and cumulative damage demands and capacities. Nonlinear seismic analysis and design of reinforced concrete buildings, Taylor and Francis, pp 23–39
- Li VC, Wang S (2002) Flexural behaviors of glass fibre-reinforced polymer (GFRP) reinforced engineered cementitious composite beams. *ACI Mater J* 99(1):11–21
- Menegotto M, Pinto PE (1973) Method of analysis for cyclically loaded reinforced concrete plane frames including changes in geometry and nonelastic behaviour of elements under combined normal force and bending. In: Proceedings IABSE symposium on resistance and ultimate deformability of structures acted on by well defined repeated loads, Lisbon
- MIDAS/Gen (2012) Analysis manual for MIDAS/GEN. MIDAS Information Technology Co., Ltd., Seoul
- Minelli F, Plizzari GA (2013) On the effectiveness of steel fibres as shear reinforcement. *ACI Struct J* 110(3):379–390
- Mishra DK, Li VC (1995) Performance of a ductile plastic hinge design with an Engineered Cementitious composite. UMCEE Report, 95-06
- Mwafy AM, Elnashai AS (2001) Static pushover versus dynamic collapse analysis of RC buildings. *Eng Struct* 23(5):407–424

- Newmark NM, Hall WJ (1982) Earth spectra: engineering monographs on earthquake criteria, structural design, and strong motion records. Earthquake Engineering Research Institute Monograph, Berkeley, CA
- Parra-Montesinos GJ, Peterfreund SW, Chao SH (2005) Highly damage-tolerant beam–column joints through use of high-performance fibre-reinforced cement composites. *ACI Struct J* 102(3):487–495
- Priestley MJN, Paulay T (1992) Seismic design of reinforced concrete and masonry buildings. Wiley, New York
- Rota M, Zuccolo E, Taverna L, Corigliano M, Lai CG, Penna A (2012) Mesozonation of the Italian territory for the definition of real spectrum-compatible accelerograms. *Bull Earthq Eng* 10(5):1357–1375
- Scott BD, Park R, Priestley MJN (1982) Stress–strain behavior of concrete confined by overlapping hoops at low and high strain rates. *ACI J Proc* 79(1):13–27
- Shannag MJ, Abu-Dyya N, Abu-Farsakh G (2005) Lateral load response of high performance fibre reinforced concrete beam–column joints. *Constr Build Mater* 19(7):500–508
- Spacone E, Filippou FC, Taucer FF (1996) Fibre beam–column model for non-linear analysis of R/C frames: part I. Formulation. *Earthq Eng Struct Dyn* 25(7):711–726
- Vasanelli E, Micelli F, Aiello MA, Plizzari G (2014) Crack width prediction of FRC beams in short and long term bending condition. *Mater Struct* 47(1–2):39–54
- Yuan F, Pan J, Xu Z, Leung CKY (2013) A comparison of engineered cementitious composites versus normal concrete in beam–column joints under reversed cyclic loading. *Mater Struct* 46(1–2):145–159